Hindawi Publishing Corporation
International Journal of Photoenergy
Volume 2012, Article ID 348292, 10 pages
doi:10.1155/2012/348292

Research Article

Synthesis, Characterization, and Photocatalytic Activity of TiO_2 Microspheres Functionalized with Porphyrin

Jin-Hua Cai,[1,2] Jin-Wang Huang,[2] Han-Cheng Yu,[2] and Liang-Nian Ji[2]

[1] *College of Chemistry and Chemical Engineering, Jinggangshan University, Jian 343009, China*
[2] *MOE Key Laboratory of Bioinorganic and Synthetic Chemistry, School of Chemistry and Chemical Engineering, State Key Laboratory of Optoelectronic Material and Technologies, Sun Yat-Sen University, Guangzhou 510275, China*

Correspondence should be addressed to Jin-Hua Cai, caijhua@mail3.sysu.edu.cn and Jin-Wang Huang, ceshjw@163.com

Received 3 January 2012; Accepted 2 February 2012

Academic Editor: Stéphane Jobic

In order to utilize visible light more efficiently in the photocatalytic reaction, TiO_2 microspheres sensitized by 5-(4-allyloxy)phenyl-10,15,20-tri(4-methylphenyl)porphyrin (APTMPP) were prepared and characterized by X-ray diffraction (XRD), X-ray photoelectron spectroscopy (XPS), nitrogen physisorption, scanning electron microscopy (SEM), Fourier transform infrared spectroscopy (FT-IR) and UV-vis diffuse reflectance spectroscopy, and so forth, The characterization results indicated that APTMPP-MPS-TiO_2 was composed of the anatase crystal phase. The morphology of the composite materials was spheriform with size of 0.3–0.7 μm and the porphyrin was chemisorbed on the surface of TiO_2 through a Si–O–Ti bond. The photooxidation of α-terpinene was employed as the model reaction to evaluate the photocatalytic activity of APTMPP-MPS-TiO_2 microspheres under visible light. The results indicated that the photodegradation of α-terpinene was significantly enhanced in the presence of the APTMPP-MPS-TiO_2 compared with the nonmodified TiO_2 under visible light.

1. Introduction

The application of semiconductors in heterogeneous photocatalysis to eliminate various pollutants in aqueous systems has gained significant attention in the last decade [1–3]. TiO_2 is considered a preferred and potential semiconductor photocatalytic material for applications requiring antimicrobial and sterilizing characteristics because some of its forms have reasonable photoactivity. Besides, it has many advantages such as inexpensiveness, easy production, (photo)chemical and biological stability, and innocuity to the environment and to human beings. It has been used for water remediation being effective for the photodegradation of many harmful organic pollutant to innocuous inorganic species [4–7]. However, some drawbacks limit its application especially in the large-scale industry. One important disadvantage of pure titania is characterized by low quantum efficiency because of high bandgap energy (~3.2 eV) and high rate of e^- and h^+ recombination. The light absorption region of anatase-typed TiO_2 particles does not fit with the solar spectrum because the solar energy above 3.0 eV ($\lambda \leq 410$ nm) only makes up less than 5% of whole sunlight. Therefore, the development of low-bandgap photoactive material, the so-called visible light photocatalyst, is strongly urged for solving environmental problems. To overcome this problem, different approaches have been proposed in the literature in which the response of the semiconductor was extended toward the visible region. Narrowing the bandgap is an effective way to enhance the photocatalytic performance of titania, and this can be done with metals and nonmetals ion doping [8–10], ion implantation, and photosensitization [11–15]. Among them, dye sensitization is considered to be an efficient method to modify the photoresponse properties of TiO_2 particles [16–18]. The dyes used are erythrosine B, rose bengal, porphyrin, and so forth. Similarly to other photosensitizers, porphyrins are recognized to be the most promising sensitizers. They not only can be involved in the reaction mechanism by transferring electrons to the conduction band of TiO_2 or to adsorbed O_2, but also they can cooperate with TiO_2 participating in photooxidation reactions by means of a direct activation of O_2 [19–24]. Recently, the photocatalytic activity of TiO_2 powders

impregnated with copper porphyrins used as sensitizers for the decomposition of 4-nitrophenol has been investigated [25–28]. But Some of them suffer from a reversible binding and the support is broken during the washing of the solvent under working conditions. A useful means to avoid these limitations is to establish the stable covalent binding between porphyrins and TiO_2 samples.

We recently reported efficient photooxidations using heterogeneous photosensitizers prepared by the covalent immobilization of metal-free porphyrins on silica microspheres [29]. To further study the photosensitization of metal-free porphyrins, one novel metal-free porphyrin derivatives, that is, 5-(4-allyloxy)phenyl-10,15,20-tri(4-chlorophenyl)porphyrin was synthesized and characterized. The catalytic activity of metal-free porphyrin complex covalent binding to TiO_2 is studied upon irradiation the sample with visible light. The oxidation of α-terpinene has been chosen as a model reaction. The purpose of this paper is to study the structural relationship between porphyrin complex and TiO_2 in the prepared composite by sol-gel processing. Furthermore, the stability of photocatalysts was also investigated and discussed.

2. Experimental Section

2.1. Materials and Chemicals. 5-(4-hydroxyl)phenyl-10, 15,20-tri(4-methylphenyl)porphyrin (HPTMPP) was synthesized in our laboratory according to [30, 31], 3-mercaptopropyltrimethoxysilane (MPS, 95.8%), tetraethyl orthosilicate, and allyl bromide (96%) were purchased from Guangzhou Jun-ye Chemistry plant. α-terpinene was obtained from Aldrich without further purification. Silica gel used to purify porphyrin by chromatograph was obtained from Qingdao. Toluene and acetonitrile were dried with calcium hydride and redistilled. All other reagents and solvents were obtained from commercial sources and used without further purification.

2.2. Physical Measurements. The scanning electron microscopy (SEM) was performed with a JSM-6330F Field Emission Scanning Electron Microscope. The XRD curves were got from Rigaku D/max 2550 VB/PC (Japan). The surface property of samples was characterized by X-ray photoelectron spectroscopy (XPS) on a PerkinElmer PHI 1600 ESCA system. The specific surface areas of the samples were measured using nitrogen adsorption method at 77 K and the Brunauer-Emmett-Teller (BET) analysis using a Flow Sorb 2300 apparatus (Micromeritics International). The pore size distributions were calculated with the DFT Plus software (Micromeritics), applying the Barrett-Joyner-Halenda (BJH) model considering cylindrical geometry of the pores. Thermal analysis was performed with a Netzsch TG-209 Thermogravimetric Analyzer. UV-vis and IR spectra were recorded on a Shimadzu UV-3150 spectrophotometer and an EQUINOX 55 Fourier transformation infrared spectrometer, respectively. Diffuse reflectance spectra in the 200–800 nm were obtained by using a Shimadzu UV-3150 UV-vis spectrophotometer. ^{1}H NMR spectra were recorded on a 300 MHz Bruker-AMX spectrophotometer with tetramethylsilane (TMS) as internal reference. Mass spectrometry analysis was performed on a Thermo LCQDECA-XP spectrometer. An iodine tungsten lamp (200W, Shanghai), ITL, was used as a light source. A distance of about 5 cm between the lamp and reactor was maintained.

2.3. Synthesis of TiO_2 Microspheres Functionalized with APTMPP (APTMPP-MPS-TiO_2). The strategy to prepare TiO_2 microspheres functionalized with APTMPP (APTMPP-MPS-TiO_2) is shown in Scheme 1.

2.3.1. Synthesis of APTMPP-MPS. APTMPP-MPS was synthesized by the reaction of 5-(4-allyloxy)phenyl-10,15,20-tri(4-methylphenyl)porphyrin (APTMPP) with 3-Mercaptopropyltrimethoxysilane (MPS), and APTMPP was prepared by the method similar to a previously reported method [32]. A mixture of 5-(4-hydroxyl)phenyl-10,15,20-tri(4-methylphenyl)porphyrin (HPTMPP) (0.6 mmol), allyl bromide (0.8 mmol), and anhydrous K_2CO_3 (1.5 g) in DMF (40 mL) was stirred for 12 h at room temperature. The reaction mixture was poured into water (150 mL) and filtered. The residue was submitted to column chromatography on silica gel using the chloroform as an eluent. The first band was collected and the solvent was evaporated. Purple solid APTMPP was obtained in 80% yield. ES-MS [$CHCl_3$, m/z]: 713[M^+]. ^{1}H NMR (300 MHz, $CDCl_3$), d: −2.68 (s, 2H, NH pyrrole), 8.88 (s, 8H, β-pyrroles), 8.11 (d, 8H, 2,6-phenyl), 7.61(d, 6H, 3,5-phenyl), 7.29 (d, 2H, 3,5-phenyl), 6.21–6.34 (t, 1H, =CH–), 5.62 (d, 1H, H–C=C–), 5.45 (1H, H–C=C–), 4.81 (2H, =C–CH_2–O), 2.73 (s, 9H, –CH3).

A mixture of MPS (40 mg, 0.2 mmol), APTMPP (143 mg, 0.2 mmol), toluene(15 mL), and 10 mg 2,20-azobis-isobutyronitrile (AIBN) was degassed and sealed under nitrogen. Then, the solution was stirring at 75°C. The progress of the reaction was monitored by TLC (chloroform as eluent). After completion of the reaction, the solvent was removed *in vacuo* and the pasty residue was washed with cold hexane, then a purple oil of APTMPP-MPS was obtained. ES-MS [$CHCl_3$, m/z]: 908[M^+], ^{1}H NMR (300 MHz, $CDCl_3$), d: −2.71 (s, 2H, NH pyrrole), 8.87 (s, 8H, β-pyrroles), 8.10 (d, 8H, 2,6-phenyl), 7.55 (d, 6H, 3,5-phenyl), 7.28 (d, 2H, 3,5-phenyl), 4.35 (2H, H_7), 3.63 (9H, H_1), 2.89 (2H, H_5), 2.73(s, 9H, –CH_3), 2.35 (2H, H_4), 2.27 (2H, H_6), 1.30 (2H, H_3), 0.89 (2H, H_2).

2.3.2. Synthesis of APTMPP-MPS-TiO_2. TiO_2 microspheres were prepared by sol-gel processes [33]. 10 mL of $Ti(OBu)_4$ is dissolved in 10 mL of anhydrous C_2H_5OH (99.7%) to produce $Ti(OBu)_4$-C_2H_5OH solution. Meanwhile, 5 mL of water and 3 mL ammonia were added to another 10 mL of anhydrous C_2H_5OH in turn to form an ethanol-NH_3-water solution. After the two resulting solutions are stirred for 30 min, respectively, the $Ti(OBu)_4$-C_2H_5OH solution is slowly added dropwise to the ethanol-NH_3-water solution under vigorously stirring to carry out a hydrolysis. Thus, a semitransparent sol is gained after continuously stirring for 1 h. Then, 2 mL ammonia was added into the mixture

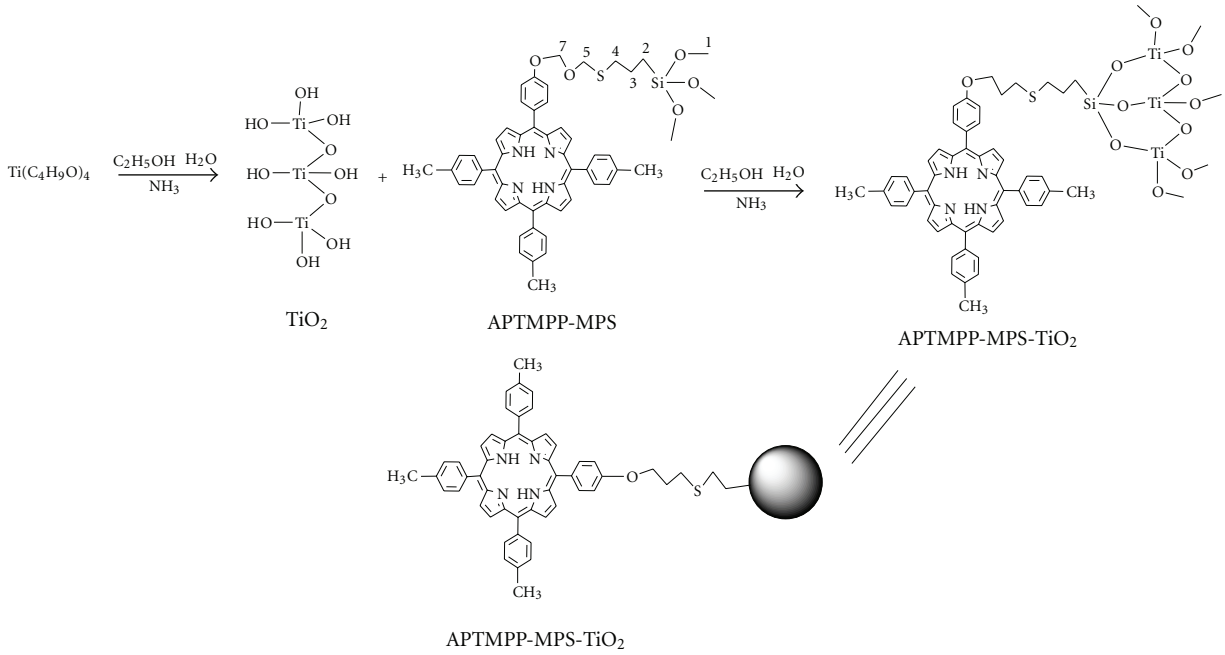

Scheme 1: Synthesis route of APTMPP-MPS-TiO_2.

(pH 11) and the solution was stirred vigorously another 12 h at room temperature. After completion of the reaction, the resulting precipitate was collected by centrifugation, washed repeatedly with alcohol, and then dried in a vacuum and white powder was obtained. To complete the surface modification with APTMPP-MPS, 40 mg APTMPP-MPS was dissolved in 30 mL of $CHCl_3$ and 1 g finely TiO_2 powder was transferred into a weighing bottle. Subsequently, After ultrasonication for 2 min and stirring for 20 min vigorously, the mixture bottle was kept at 80°C in the water bath to vaporize the liquid under stirring. The product was washed with $CHCl_3$ in a Soxhlet extractor overnight to remove unbound APTMPP. Finally, the solids were dried at 110°C for 12 h. Unbound APTDCPP was quantified through spectrophotometric measurement at 518 nm, by using a calibration curve obtained by using a suitably diluted solution. Thus, the amounts of bound porphyrins were determined by difference between the two measurements. APTMPP in APTMPP-MPS-TiO_2 was 0.0202 mmol/g obtained by this method.

2.4. Photocatalytic Activity Tests. Photooxidation experiments of α-terpinene were carried out in a 30 mL self-designed jacketed reactor maintained at a certain temperature by circulation of thermostated water [29, 34]. In a typical experiment, aqueous slurries were prepared by adding a certain amount of TiO_2 or APTMPP-MPS-TiO_2 to 20 mL solution containing α-terpinene at 3.7×10^{-4} M. Irradiations were performed with a 200 W iodine tungsten lamp in which the UV light was filtered by a 410 nm cut filter. The aqueous slurries were stirred and bubbled with humid oxygen for 10 min prior to the irradiation. At 10 min intervals, the dispersion was extracted and centrifuged to separate the photocatalyst particles. The concentration of α-terpinene was analyzed by UV-vis spectroscopy. The photodegradation percentage of α-terpinene can be calculated using the changes of the absorbance of α-terpinene at 265 nm. The reaction products were purified by extraction from the reaction mixtures. ESMS [$CHCl_3$, m/z]: 168 (M^+).δ 0.98~1.00 (d, 6H CH_3), 1.36 (s, 3H, CH_3), 1.51~1.56 (2H, methylene, CH_2), 1.89~2.04 (2H, methylene, CH_2), 1.93 (H, isopropyl, CH), 6.37~6.49 (d, 4H, olefinic, CH) [35].

2.5. Approach of Calculation. The degradation rate of α-terpinene in the reaction process could be calculated by the following formula:

$$\text{decolorization rate} = \frac{(A_0 - A_t)}{A_0} \times 100\%, \quad (1)$$

where A_t is the absorbance of α-terpinene measured at 265 nm at time t, and A_0 is the initial absorbance prior to reaction. The residual concentrations of α-terpinene could be calculated by the following formula:

$$C_t = \frac{A_t}{A_0} \times C_0, \quad (2)$$

where C_t is residual concentration of α-terpinene at time t and C_0 is the initial concentration of α-terpinene.

3. Results and Discussion

3.1. Preparation and Characterization of APTMPP-MPS-TiO_2. The strategy used to prepare TiO_2 microspheres functionalized with porphyrin is shown in Scheme 1. The porphyrin was immobilized on the TiO_2 microspheres

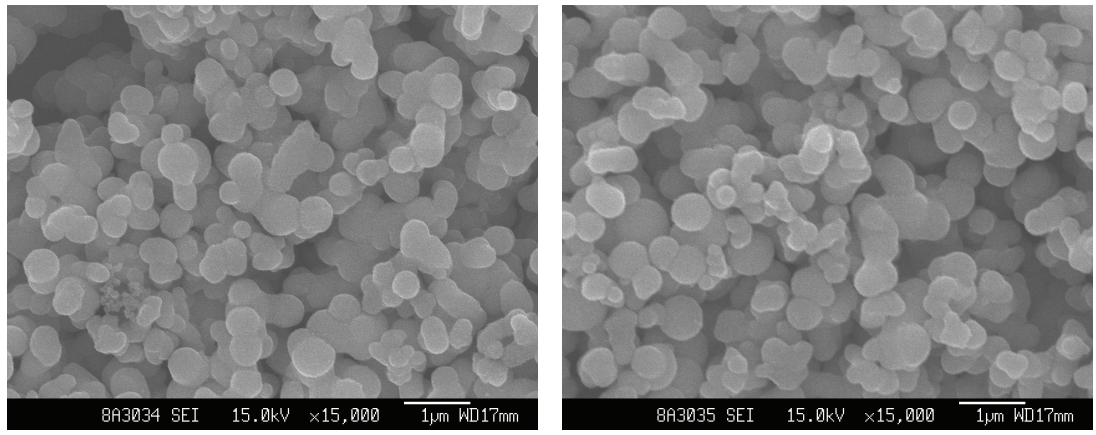

(a) (b)

Figure 1: Scanning electron micrograph of TiO_2 (a) and APTMPP-MPS-TiO_2 (b).

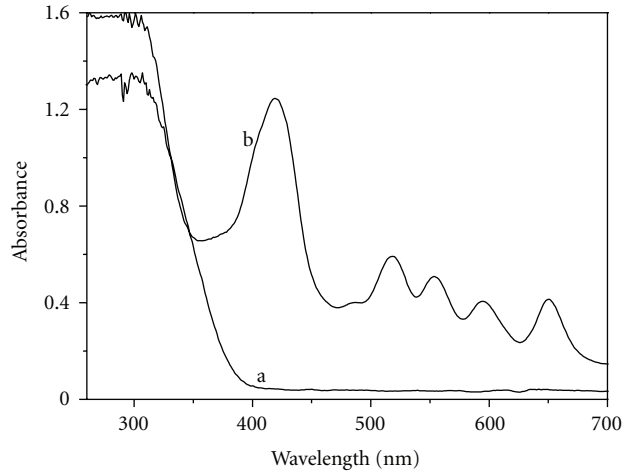

Figure 2: UV-vis DRS spectra of TiO_2 (a) APTMPP-MPS-TiO_2 (b).

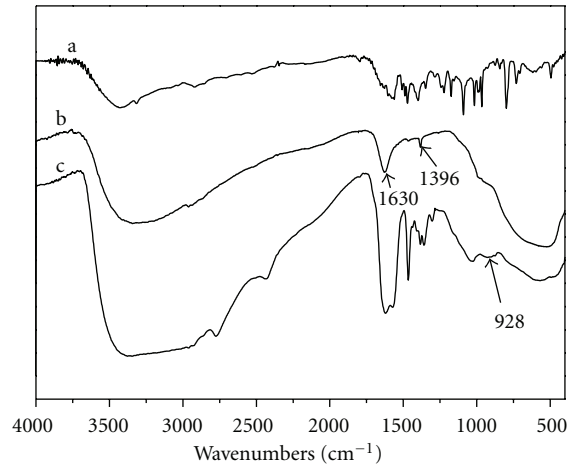

Figure 3: FT-IR spectra of APTMPP-MPS (a), TiO_2 (b), APTMPP-MPS-TiO_2(c).

by the condensation reaction of APTMPP-MPS and TiO_2 microspheres.

The morphology of TiO_2 and APTMPP-MPS-TiO_2 was obtained by scanning electron micrograph as shown in Figure 1. The micrograph shows irregularly shaped spherical particles with loose and discrete structure. Distribution of particle size of TiO_2 and APTMPP-MPS-TiO_2 over a broad range was observed with the average size of 0.7 μm. No change has happened in the diameter of TiO_2 after APTMPP bonding on it.

The UV-vis DRS spectra of APTMPP-MPS-TiO_2 and pure TiO_2 are shown in Figure 2. It is worth noting that no shift of the bandgap edge of TiO_2 can be observed in loaded sample. APTMPP-MPS-TiO_2 exhibits typical porphyrin absorption features with a strong Soret band at 419 nm and moderate Q bands at 519, 552, 595, and 650 nm, the strong band appears at 419 nm arising from the transition of $a_{1u}(\pi)$–$e_g(\pi)$, and the less intense bands in the 500–650 nm region corresponding to the $a_{2u}(\pi)$–$e_g(\pi)$ transition attributed to porphyrin [36] while there is no absorption above 400 nm for pure TiO_2. It can be found that APTMPP-MPS-TiO_2 composites exhibit a broader absorption range than pure TiO_2.

Figure 3 shows the FT-IR spectra of APTMPP-MPS-TiO_2. The peak around 1630 cm^{-1} is due to the bending vibration of the O–H bond of chemisorbed water, and the peak around 3400 cm^{-1} is due to the stretching mode of the O–H bond of free water. The IR band at 400–850 cm^{-1} and 1400 cm^{-1} corresponds to the Ti–O–Ti stretching vibration mode in crystal TiO_2. Unlike the pure TiO_2 [37], the modified TiO_2 samples have a new broad IR band at about 928 cm^{-1} corresponding to the vibrations of Ti–O–Si bonds [38]. The existence of Ti–O–Si bond verifies the formation of chemical bonding between titania and organic component. That at around 1000 cm^{-1} is assigned to symmetric and asymmetric Si–O–Si stretching vibrations in siloxane network. Some new bands between 1300 and 1400 cm^{-1} attributed to the pyrrole C=N stretching also indicate that the presence of porphyrins in the hybrid materials.

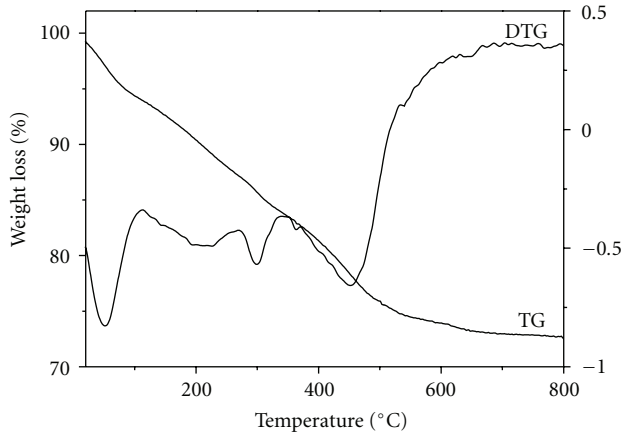

Figure 4: TG-DTG curve for APTMPP-MPS-TiO_2.

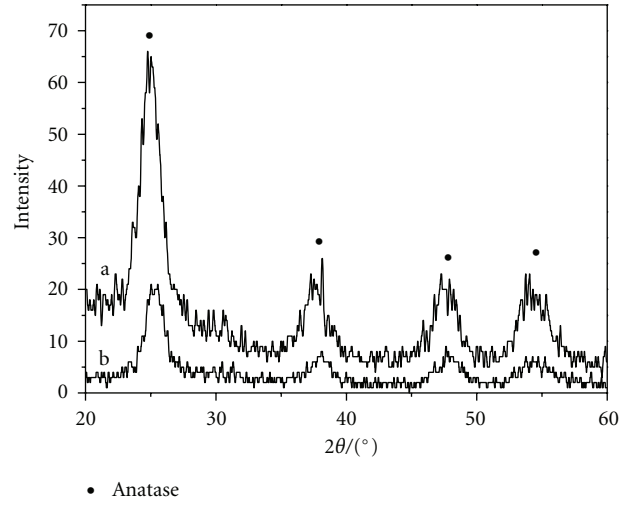

Figure 5: XRD spectra of TiO_2 (a), APTMPP-MPS-TiO_2 (b).

Figure 4 shows the TG and DTG for APTMPP-MPS-TiO_2 sample. From the TG-DTG analysis of the APTMPP-MPS-TiO_2, the weight of particles sharply decreases up to 450°C and slowly decreases from 450 to 800°C. TG-DTG analysis of the sample also shows the endothermic peak at 100°C and two exothermic peaks at 290 and 450°C. It is thought that the peak at 100°C is due to free adsorbed water, and the peak at 290°C is due to the decomposition of the porphyrin and residual hydroxy group. In addition, the peak at 450°C corresponds to the crystallization of the amorphous phase into the anatase phase. Above 650°C, it can be assumed that the product completely transforms into the anatase phase because there is no change in particle weight.

From the X-ray diffraction patterns of the samples shown in Figure 5, we can see only that the anatase crystalline phase was present in both samples. The major phase of the photocatalyst is pure anatase without brookite. No rutile peaks were observed for all titania. The peaks appearing at $2\theta = 25.3°$, 38.7°, 47.6°, and 54.8° are attributed to anatase phase. It was confirmed that $Ti(OC_4H_9)_4$ was oxidized into TiO_2, and the formed TiO_2 was mostly anatase by the calcination in the air. In addition, immobilization of APTMPP-MPS on TiO_2 has little effects on the interlayer spacing. This demonstrates that the porphyrins grafted on TiO_2 surface does not crystallize.

Figure 6 shows the nitrogen adsorption-desorption curves measured by BET method and the pore-size distribution calculated from desorption isotherms of APTMPP-MPS-TiO_2 prepared by sol-gel method. As seen, the isotherm of the modified sample shows a combination of type I [39]. At low relative pressure, the isotherm exhibits high adsorption, indicating that as-prepared samples contain micropores (type I). While at high relative pressure from 0.6 to 1.0, the curve exhibits a little biger adsorption, indicating the bigger crystallites aggregation form bigger pores. The BET surface area and specific pore volume of the composite are 266.3 $m^2\,g^{-1}$ and 0.23 $cm^3\,g^{-1}$. Figure 7 shows the pore size distribution curve of the corresponding products by the BJH method. It can be seen that the diameter of pore ranged from 1.8 to 4.0 nm, and the largest pore diameter was 2.1 nm.

In order to analyze the chemical composition of the APTMPP-MPS-TiO_2, we performed X-ray photoelectron spectroscopy (XPS) analyses. Figure 8 shows XPS survey spectrum for the surface of APTMPP-MPS-TiO_2 particles. The XPS spectrum reveals characteristic peaks from Ti, C, Si, S, N, and oxygen. Parameters of the XPS peak for Ti($2P_{3/2}$) and O(1S) are listed in Table 1. The peaks of APTMPP-MPS-TiO_2 are shifted to higher binding energies by 0.28 and 0.62 eV for Ti($2P_{3/2}$) and O(1S) than TiO_2 [40], respectively. The increase of binding energy for Ti($2P_{3/2}$) and O(1S) while APTMPP-MPS adsorbed on TiO_2 indicates chemical bonding at the interface of the silica coating layer and titania particle surface. Figure 9 shows the XPS spectra of O(1S) peak for APTMPP-MPS-TiO_2. The shape of a wide and asymmetric peak of XPS O(1S) spectra indicated that there would be more than one chemical state according to the binding energy. It includes crystal lattice oxygen (O_{Ti-O} or O_{Si-O}) and chemisorbed oxygen (O_{O-H}). The main contribution is attributed to Ti–O in TiO_2, and the other two kinds of oxygen contributions can be ascribed to the –OH in Ti–OH and the Si–O in SiO_2, respectively [41, 42]. Usually, hydroxyl groups measured by XPS are ascribed to the chemisorbed water. As seen, the hydroxyl content increased in the sample. This is probably due to the fact that the films easily adsorb water vapor in air, leading to the formation of hydroxyl on the films. This also corresponds to the results of previous TG and FTIR.

3.2. Photocatalytic Activity of APTMPP-MPS-TiO_2

3.2.1. α-Terpinene Photooxidation. The photocatalytic activities for the degradation of α-terpinene under visible light irradiation using prepared photocatalysts were tested. α-terpinene degradation occurred promptly in the visible irradiation under the adding of the APTMPP-MPS-TiO_2 as confirmed by the UV-vis spectra changes of APTMPP-MPS-TiO_2 (Figure 10). The absorption spectrum of α-terpinene in ethanol was characterized by the band of 265 nm in

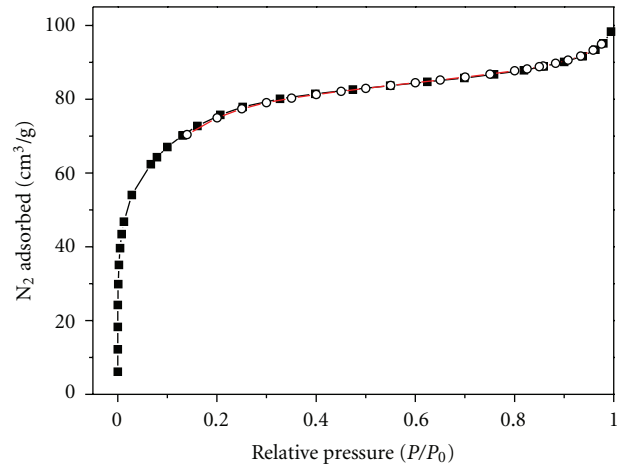

Figure 6: Nitrogen adsorption isotherms of APTMPP-MPS-TiO_2.

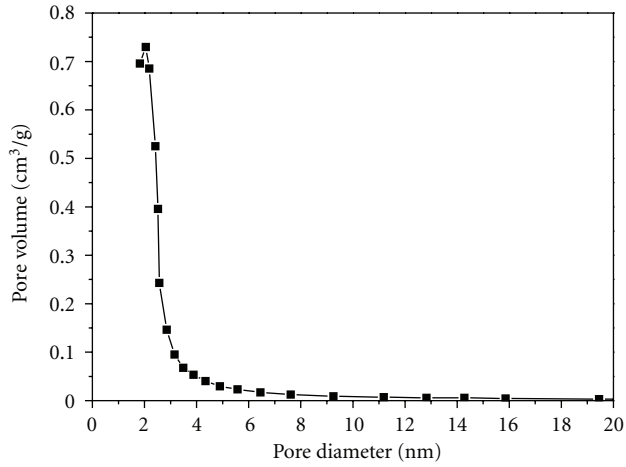

Figure 7: Pore diameter distribution of APTMPP-MPS-TiO_2.

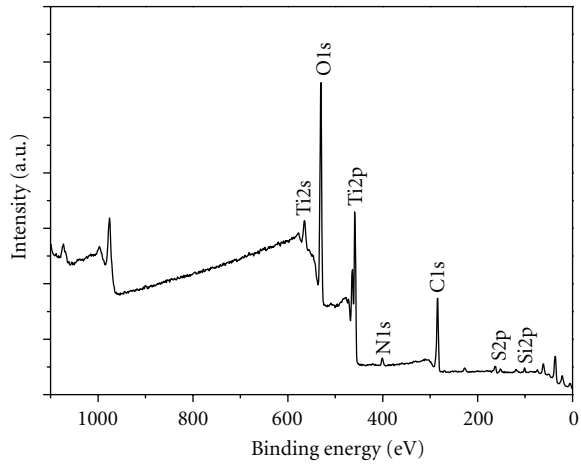

Figure 8: XPS survey spectrum for the surface of APTMPP-MPS-TiO_2.

Table 1: XPS data for APTCPP-MPS-TiO_2.

Orbit	Binding energy (eV)	FEHM	Content (atom%)
Ti2p3/2	458.76	1.16	16.56
C1s	284.82	1.87	27.99
O1s	530.28	1.38	49.41
Si2p	101.48	1.36	1.96
S2p	163.29	1.97	1.62
N1s	401.94	1.51	6.46

FWHM: full width at a half of the maximum height of peaks. BE: binding energy.

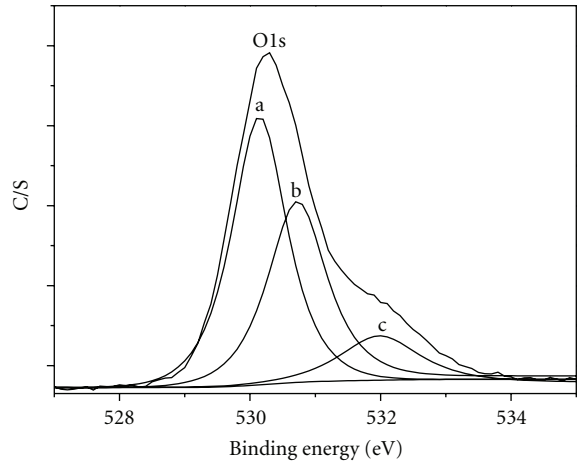

(a) 529.9 eV O1s (Ti–O)
(b) 530.9 eV O1s (–OH)
(c) 532.4 O1s (Si–O)

Figure 9: XPS spectra of O1s peak for APTMPP-MPS-TiO_2.

the UV-vis region. As observed in Figure 10, the intensity of the 265 nm absorption band decreased rapidly under visible light irradiation, indicating the degradation of α-terpinene in the presence of APTMPP-MPS-TiO_2 microspheres. For comparison, blank experiments, in which the photooxidation experiment of α-terpinene was performed in dark in the presence of APTMPP-MPS-TiO_2 or irradiated with visible light with TiO_2, were done and no obvious catalytic results were observed. It believes that both visible light and APTMPP-MPS-TiO_2 were indispensable to the photooxidation of α-terpinene.

A tentative photocatalytic mechanism of APTMPP-MPS-TiO_2 was deduced and shown in Scheme 2. When the visible light irradiates on the surface of APTMPP-MPS-TiO_2, the porphyrin molecules adsorbed on the surface of TiO_2 can be excited by visible light, and then the photoinduced electrons inject into the conduction band of TiO_2. Subsequently, the reactive electrons in the conduction band can reduce O_2 adsorbed on the surface of TiO_2 to O_2^-, which can further transform into H_2O_2 and $^\bullet OH$, resulting in the oxidation of α-terpinene.

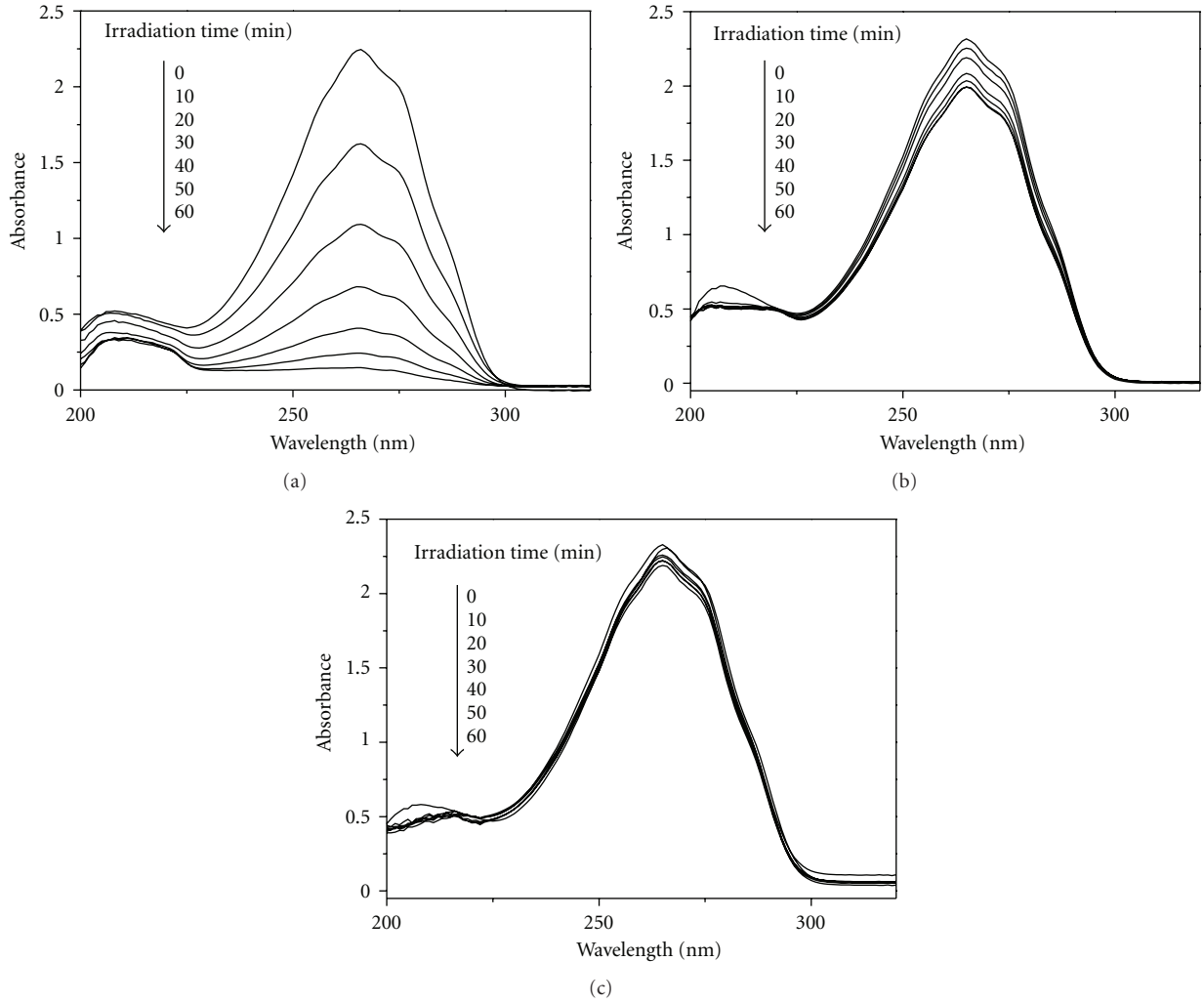

Figure 10: The temporal UV-vis spectral changes of α-terpinene (3.7×10^{-4} M): (a) under visible irradiation with APTMPP-MPS-TiO_2 (1.0 mg/mL), (b) under visible irradiation with TiO_2 (1.0 mg/mL), (c) dark reaction with APTMPP-MPS-TiO_2 (1.0 mg/mL).

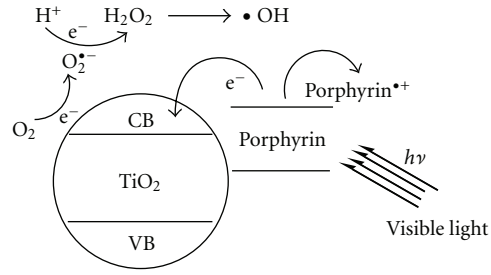

Scheme 2: Tentative mechanism of α-terpinene photooxidation on the surface of APTMPP-MPS-TiO_2.

3.2.2. Effect of Catalyst Amount on the Photocatalytic Activity. The photocatalytic activities are also influenced by the catalyst amount, as shown in Figure 11. It reveals that APTMPP-MPS-TiO_2 hybrids have higher photocatalytic activity than that of only TiO_2 particles and the photooxidation efficiency increases with an increase in APTMPP-MPS-TiO_2 concentration up to 2.0 mg/mL and then remains almost constant above a certain level. This has been explained as the concentration of the APTMPP-MPS-TiO_2 increased; the number of photons absorbed and the number of α-terpinene molecules adsorbed increased with respect to an increase in the number of APTMPP-MPS-TiO_2 molecules. The density of the molecule in the area of illumination also increases and thus the rate gets enhanced. After a certain level, the dye

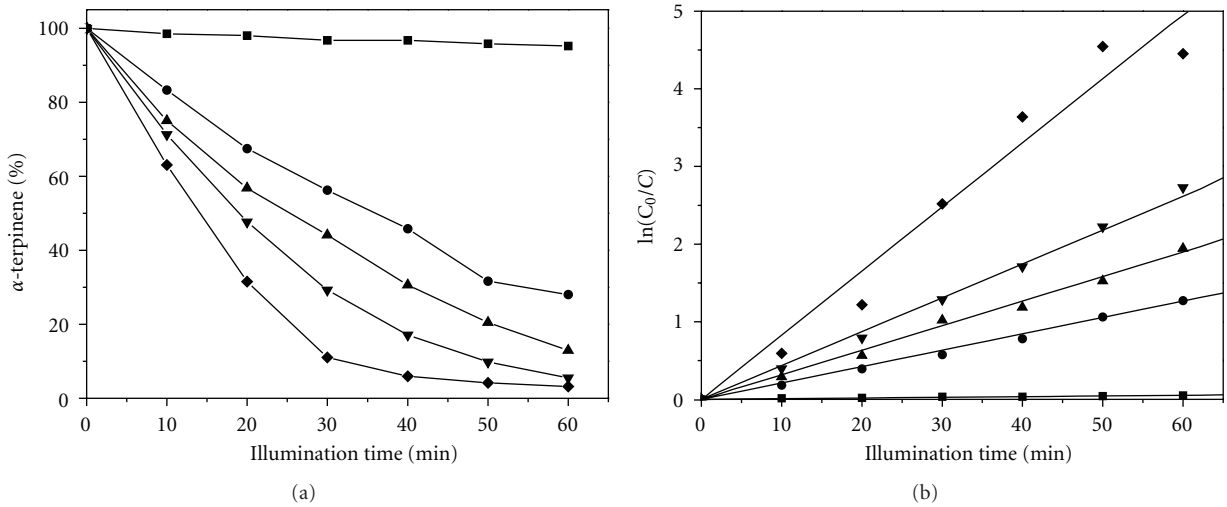

Figure 11: (a) Effect of catalyst amount on the photooxidation of α-terpinene (b)The pseudo-first-order photocatalysis rate constants of α-terpinene (■) TiO_2(1 mg/mL) and APTMPP-MPS-TiO_2 (•) 0.5 mg/mL (▲) 1 mg/mL (▼) 1.5 mg/mL (♦) 2 mg/m.

molecules available are not sufficient for adsorption by the increased number of catalyst molecule. Hence, the additional catalyst powder is not involved in the photocatalytic activity and the rate does not increase with increase in the amount of catalyst beyond certain limit. Replotting Figure 11(a) in the $\ln(C_0/C_t)-t$ coordinates (Figure 11(b)). It is found that α-terpinene's photooxidation follows the pseudo-first-order kinetic in the lower initial APTMPP-MPS-TiO_2 amount (0.5–1.5 mg/mL). However, when APTMPP-MPS-TiO_2 amount was greater than 1.5 mg/mL, the photocatalytic oxidation would deviate from the pseudo-first-order kinetic with respect to APTMPP-MPS-TiO_2 amount.

3.2.3. Stability and Reusability of the Catalysts. For the assessment of catalyst stability and reusability, APTMPP-MPS-TiO_2 sample was used in the degradation of different solutions of α-terpinene in four consecutive experiments. Catalyst was recovered using centrifuge during sampling and after each experiment. The UV-vis and IR spectra as well as the morphology of the recovered hybrid material did not show any substantial change compared to fresh material. All reaction solutions analyzed after catalytic reactions did not show the characteristic soret band of porphyrins, which indicated that no APTMPP lost from TiO_2. Using the recovered APTMPP-MPS-TiO_2 as catalyst to catalyze α-terpinene photooxidation in the same conditions, they retain their high catalytic activity after being recycled four times. For example, the photooxidation percentages of α-terpinene for four consecutive experiments are as follows: 87, 84, 80, 79, and 81% in the same conditions (1 mg/mL APTMPP-MPS-TiO_2, 3.7×10^{-4} M α-terpinene, 60 min). These results indicate that APTMPP-MPS-TiO_2 has highly chemical stability and is recoverable and reusable.

4. Conclusions

In this work, novel APTMPP-MPS-TiO_2 hybrids with high photocatalytic activity were synthesized by immobilizing metal-free porphyrin on titania sol particles. The metal-free porphyrin can extend the light absorption of TiO_2 into visible region and make α-terpinene be effectively photooxidated under visible light. The degradation reaction process of α-terpinene completely obeys the first-order law. Furthermore, the photocataysts are stable, harmless, and they can be reused with high efficiency.

Acknowledgments

The authors are grateful to the supports of Guangzhou Municipality Science and Technology Bureau of China, the National Natural Science Foundation of China and National Key Foundation Research Development Project (973) Item of China (no. 2007 CB815306), the foundation for Doctors of Jianggangshan University (JZ10044), the Education Department Foundation of the Guangxi Zhuang Autonomous Region of China (201012MS203), the Education Department Foundation of the Jiangxi Province (GJJ12472), and the Young Science Foundation of Guangxi Province of China (0832090).

References

[1] S. U. M. Khan, M. Al-Shahry, and W. B. Ingler, "Efficient photochemical water splitting by a chemically modified n-TiO_2," *Science*, vol. 297, no. 5590, pp. 2243–2245, 2002.

[2] M. R. Hoffmann, S. T. Martin, W. Choi, and D. W. Bahnemann, "Environmental applications of semiconductor photocatalysis," *Chemical Reviews*, vol. 95, no. 1, pp. 69–96, 1995.

[3] A. L. Linsebigler, G. Lu, and J. T. Yates, "Photocatalysis on TiO_2 surfaces: principles, mechanisms, and selected results," *Chemical Reviews*, vol. 95, no. 3, pp. 735–758, 1995.

[4] D. C. Schmelling and K. A. Gray, "Photocatalytic transformation and mineralization of 2,4,6-trinitrotoluene (TNT) in TiO_2 slurries," *Water Research*, vol. 29, no. 12, pp. 2651–2662, 1995.

[5] J. Hong, C. Sun, S. G. Yang, and Y. Z. Liu, "Photocatalytic degradation of methylene blue in TiO_2 aqueous suspensions using microwave powered electrodeless discharge lamps," *Journal of Hazardous Materials*, vol. 133, no. 1–3, pp. 162–166, 2006.

[6] G. Zhanqi, Y. Shaogui, T. Na, and S. Cheng, "Microwave assisted rapid and complete degradation of atrazine using TiO_2 nanotube photocatalyst suspensions," *Journal of Hazardous Materials*, vol. 145, no. 3, pp. 424–430, 2007.

[7] R. D. Barreto, K. A. Gray, and K. Anders, "Photocatalytic degradation of methyl-tert-butyl ether in TiO_2 slurries: a proposed reaction scheme," *Water Research*, vol. 29, no. 5, pp. 1243–1248, 1995.

[8] S. Yang, Y. Guo, N. Yan et al., "Remarkable effect of the incorporation of titanium on the catalytic activity and SO_2 poisoning resistance of magnetic Mn-Fe spinel for elemental mercury capture," *Applied Catalysis B*, vol. 101, no. 3-4, pp. 698–708, 2011.

[9] Y. Xie, Y. Li, and X. Zhao, "Low-temperature preparation and visible-light-induced catalytic activity of anatase F-N-codoped TiO_2," *Journal of Molecular Catalysis A*, vol. 277, no. 1-2, pp. 119–126, 2007.

[10] Y. H. Xu and Z. X. Zeng, "The preparation, characterization, and photocatalytic activities of Ce-TiO_2/SiO_2," *Journal of Molecular Catalysis A*, vol. 279, no. 1, pp. 77–81, 2008.

[11] C. C. Yen, D. Y. Wang, M. H. Shih, L. S. Chang, and H. C. Shih, "A combined experimental and theoretical analysis of Fe-implanted TiO_2 modified by metal plasma ion implantation," *Applied Surface Science*, vol. 256, no. 22, pp. 6865–6870, 2010.

[12] A. Ghicov, J. M. Macak, H. Tsuchiya et al., "Ion implantation and annealing for an efficient N-doping of TiO_2 nanotubes," *Nano Letters*, vol. 6, no. 5, pp. 1080–1082, 2006.

[13] J. K. Park, H. R. Lee, J. Chen, H. Shinokubo, A. Osuka, and D. Kim, "Photoelectrochemical properties of doubly β-functionalized porphyrin sensitizers for dye-sensitized nanocrystalline-TiO_2 solar cells," *Journal of Physical Chemistry C*, vol. 112, no. 42, pp. 16691–16699, 2008.

[14] H. Shen, L. Mi, P. Xu, W. Shen, and P. N. Wang, "Visible-light photocatalysis of nitrogen-doped TiO_2 nanoparticulate films prepared by low-energy ion implantation," *Applied Surface Science*, vol. 253, no. 17, pp. 7024–7028, 2007.

[15] M. C. Neves, J. M. F. Nogueira, T. Trindade, M. H. Mendonça, M. I. Pereira, and O. C. Monteiro, "Photosensitization of TiO_2 by Ag_2S and its catalytic activity on phenol photodegradation," *Journal of Photochemistry and Photobiology A*, vol. 204, no. 2-3, pp. 168–173, 2009.

[16] A. Kathiravan and R. Renganathan, "Effect of anchoring group on the photosensitization of colloidal TiO_2 nanoparticles with porphyrins," *Journal of Colloid and Interface Science*, vol. 331, no. 2, pp. 401–407, 2009.

[17] O. Ozcan, F. Yukruk, E. U. Akkaya, and D. Uner, "Dye sensitized artificial photosynthesis in the gas phase over thin and thick TiO_2 films under UV and visible light irradiation," *Applied Catalysis B*, vol. 71, no. 3-4, pp. 291–297, 2007.

[18] D. Chatterjee and A. Mahata, "Visible light induced photodegradation of organic pollutants on dye adsorbed TiO_2 surface," *Journal of Photochemistry and Photobiology A*, vol. 153, no. 1–3, pp. 199–204, 2002.

[19] D. Chen, D. Yang, J. Geng, J. Zhu, and Z. Jiang, "Improving visible-light photocatalytic activity of N-doped TiO_2 nanoparticles via sensitization by Zn porphyrin," *Applied Surface Science*, vol. 255, no. 5, pp. 2879–2884, 2008.

[20] D. Li, W. Dong, S. Sun, Z. Shi, and S. Feng, "Photocatalytic degradation of acid chrome blue K with porphyrin-sensitized TiO_2 under visible light," *Journal of Physical Chemistry C*, vol. 112, no. 38, pp. 14878–14882, 2008.

[21] S.-J. Moon, E. Baranoff, S. M. Zakeeruddin et al., "Enhanced light harvesting in mesoporous TiO_2/P3HT hybrid solar cells using a porphyrin dye," *Chemical Communications*, vol. 47, no. 29, pp. 8244–8246, 2011.

[22] J. E. Kroeze, R. B. M. Koehorst, and T. J. Savenije, "Singlet and triplet exciton diffusion in a self-organizing porphyrin antenna layer," *Advanced Functional Materials*, vol. 14, no. 10, pp. 992–998, 2004.

[23] M. Y. Duan, J. Li, G. Mele et al., "Photocatalytic activity of novel tin porphyrin/TiO_2 based composites," *Journal of Physical Chemistry C*, vol. 114, no. 17, pp. 7857–7862, 2010.

[24] C.-L. Wang, Y.-C. Chang, C.-M. Lan, C.-F. Lo, E. W.-G. Diau, and C.-Y. Lin, "Enhanced light harvesting with π-conjugated cyclic aromatic hydrocarbons for porphyrin-sensitized solar cells," *Energy and Environmental Science*, vol. 4, no. 5, pp. 1788–1795, 2011.

[25] C. Wang, G. M. Yang, J. Li et al., "Novel meso-substituted porphyrins: synthesis, characterization and photocatalytic activity of their TiO_2-based composites," *Dyes and Pigments*, vol. 80, no. 3, pp. 321–328, 2009.

[26] G. Mele, R. D. Sole, G. Vasapollo et al., "TRMC, XPS, and EPR characterizations of polycrystalline TiO_2 porphyrin impregnated powders and their catalytic activity for 4-nitrophenol photodegradation in aqueous suspension," *Journal of Physical Chemistry B*, vol. 109, no. 25, pp. 12347–12352, 2005.

[27] C. Wang, J. Li, G. Mele et al., "Efficient degradation of 4-nitrophenol by using functionalized porphyrin-TiO_2 photocatalysts under visible irradiation," *Applied Catalysis B*, vol. 76, no. 3-4, pp. 218–226, 2007.

[28] G. Mele, R. Del Sole, G. Vasapollo, E. García-López, L. Palmisano, and M. Schiavello, "Photocatalytic degradation of 4-nitrophenol in aqueous suspension by using polycrystalline TiO_2 impregnated with functionalized Cu(II) -porphyrin or Cu(II)-phthalocyanine," *Journal of Catalysis*, vol. 217, no. 2, pp. 334–342, 2003.

[29] J. H. Cai, J. W. Huang, P. Zhao, Y. J. Ye, H. C. Yu, and L. N. Ji, "Silica microspheres functionalized with porphyrin as a reusable and efficient catalyst for the photooxidation of 1,5-dihydroxynaphthalene in aerated aqueous solution," *Journal of Photochemistry and Photobiology A*, vol. 207, no. 2-3, pp. 236–243, 2009.

[30] J. W. Huang, W. J. Mei, J. Liu, and L. N. Ji, "The catalysis of some novel polystyrene-supported porphyrinatomanganese(III) in hydroxylation of cyclohexane with molecular oxygen," *Journal of Molecular Catalysis A*, vol. 170, no. 1-2, pp. 261–265, 2001.

[31] B. Fu, H. C. Yu, J. W. Huang, P. Zhao, J. Liu, and L. N. Ji, "Mn(III) porphyrins immobilized on magnetic polymer nanospheres as biomimetic catalysts hydroxylating cyclohexane with molecular oxygen," *Journal of Molecular Catalysis A*, vol. 298, no. 1-2, pp. 74–80, 2009.

[32] J. H. Cai, J. W. Huang, P. Zhao, Y. J. Ye, H. C. Yu, and L. N. Ji, "Silica-metalloporphyrins hybrid materials: preparation and catalysis to hydroxylate cyclohexane with molecular oxygen," *Journal of Sol-Gel Science and Technology*, vol. 50, no. 3, pp. 430–436, 2009.

[33] J. Yan, X. Li, S. Cheng, Y. Ke, and X. Liang, "Facile synthesis of titania-zirconia monodisperse microspheres and application

for phosphopeptides enrichment," *Chemical Communications*, no. 20, pp. 2929–2931, 2009.

[34] J. H. Cai, J. W. Huang, P. Zhao, Y. H. Zhou, H. C. Yu, and L. N. Ji, "Photodegradation of 1,5-dihydroxynaphthalene catalyzed by meso-tetra(4-sulfonatophenyl)porphyrin in aerated aqueous solution," *Journal of Molecular Catalysis A*, vol. 292, no. 1-2, pp. 49–53, 2008.

[35] S. M. Ribeiro, A. C. Serra, and A. M. D. A. Rocha Gonsalves, "Immobilised porphyrins in monoterpene photooxidations," *Journal of Catalysis*, vol. 256, no. 2, pp. 331–337, 2008.

[36] E. F. Aboelfetoh and R. Pietschnig, "Preparation and catalytic performance of Al2O3, TiO_2 and SiO_2 supported vanadium based-catalysts for C-H activation," *Catalysis Letters*, vol. 127, no. 1-2, pp. 83–94, 2009.

[37] M. Zhang, L. Shi, S. Yuan, Y. Zhao, and J. Fang, "Synthesis and photocatalytic properties of highly stable and neutral TiO_2/SiO_2 hydrosol," *Journal of Colloid and Interface Science*, vol. 330, no. 1, pp. 113–118, 2009.

[38] M. Houmard, D. Riassetto, F. Roussel et al., "Morphology and natural wettability properties of sol-gel derived TiO_2-SiO_2 composite thin films," *Applied Surface Science*, vol. 254, no. 5, pp. 1405–1414, 2007.

[39] S. Zhan, D. Chen, X. Jiao, and Y. Song, "Mesoporous TiO_2/SiO_2 composite nanofibers with selective photocatalytic properties," *Chemical Communications*, no. 20, pp. 2043–2045, 2007.

[40] T. H. Meen, W. Water, W. R. Chen, S. M. Chao, L. W. Ji, and C. J. Huang, "Application of TiO_2 nano-particles on the electrode of dye-sensitized solar cells," *Journal of Physics and Chemistry of Solids*, vol. 70, no. 2, pp. 472–476, 2009.

[41] J. Xu, Y. Ao, D. Fu, and C. Yuan, "A simple route for the preparation of Eu, N-codoped TiO_2 nanoparticles with enhanced visible light-induced photocatalytic activity," *Journal of Colloid and Interface Science*, vol. 328, no. 2, pp. 447–451, 2008.

[42] J. G. Yu, H. G. Yu, B. Cheng, X. J. Zhao, J. C. Yu, and W. K. Ho, "The effect of calcination temperature on the surface microstructure and photocatalytic activity of TiO_2 thin films prepared by liquid phase deposition," *Journal of Physical Chemistry B*, vol. 107, no. 50, pp. 13871–13879, 2003.